IIETA International Information and Engineering Technology Association
Advancing the World of Information and Engineering

Mathematical Modelling of Engineering Problems
Vol. 11, No. 11, November, 2024, pp. 2892-2900
Journal homepage: http://iieta.org/journals/mmep

Numerical Modeling of Cavitation-Induced Abrasion in Ogee Spillways

Mohammed Q. Abbas*, Ali N. Hilo, Thaar S. Al-Gasham

College of Engineering, University of Wasit, Wasit 52001, Iraq

Corresponding Author Email: mohammad1992qassim@gmail.com

https://doi.org/10.18280/mmep.111102

Received: 3 May 2024
Revised: 10 August 2024
Accepted: 24 August 2024
Available online: 29 November 2024

Keywords:
ogee spillway, abrasion, cavitation, Computational Fluid Dynamics, ANSYS Fluent software

ABSTRACT

The purpose of this work is to evaluate the impacts of flow rate on cavitation and abrasion in ogee spillways using numerical simulations. One of the most complicated and frequent problems with spillway structures is abrasion. The spillway is the most crucial and delicate component of a dam. The most effective method for analyzing this significant hydraulic event is the cavitation index. Computational Fluid Dynamic (CFD) ANSYS Fluent Software was used to build a water-Air-spillway interaction model. Five different flow rates ranging from 100 m^3/s to 717 m^3/s were evaluated on the simulated model. The outcomes tell that when the flowrate increases, the cavitation increases proportionally, and thus the amount of abrasion of the spillway concrete surface increases. The spillway crest was found to have the least amount of abrasion, unlike the toe and chute of the spillway, which had a higher amount of abrasion. The results also show that higher flow rates lead to increased cavitation and abrasion, with the maximum abrasion of 1.0 mm occurring at the highest flow rate.

1. INTRODUCTION

Due to the high-pressure shock waves created when vapor cavities collapse, cavitation can cause damage to drain channels or even perforate them at high flow stream velocities [1]. Due to its capacity to efficiently and safely release extra water upstream and downstream when correctly designed and implemented, ogee sewers are frequently employed in the construction of hydraulic structures [2]. In order to gain a better understanding of ogee streams and their characteristics, it is also acknowledged that deviation from standard design variables, such as a change in upstream flow circumstances, a changed crest shape, or a change in the channel of approach due to local engineering features, can alter the flow characteristics. Because structure dams and related infrastructure is expensive, it is important to test a hydraulic model with multiple downstreams connected to different dams under certain engineering circumstances. Furthermore, if the water drainage gutter is ineffective, there might be significant property damage in addition to probable fatalities [3].

In a watershed runway model, Chanson [1] has carried out extensive research on aerators and ventilators. He said that the lumen starts off with weak nuclei. Cavitation frequently happens in mechanical and hydraulic structures, according to Kramer [4]. Low pressure and high velocities frequently occur near the edges of hydraulic structures, such as straggling blocks, manholes, and downspouts [5], and are caused by these phenomena.

Instability, including wear and abrasion, can cause system damage after cavitation has taken place. General design guidelines based on the critical cavitation index provide insights into protective measures against cavitation damage in hydraulic structures [6]. For structures with a cavitation index below 1.8, no additional protection is typically required. When the cavitation index ranges between 0.25 and 1.8, surface-level modifications, such as smoothing surface irregularities, may suffice to mitigate damage. For indices between 0.17 and 0.25, structural redesign measures, such as increasing boundary curvature, are often necessary. If the cavitation index lies between 0.12 and 0.17, air galleries can be employed to provide additional protection. However, when the cavitation index exceeds 0.12, the structure's surface cannot be effectively protected, necessitating a complete redesign of the hydraulic system [6]. These guidelines highlight the critical role of cavitation indices in ensuring the safety and durability of hydraulic structures.

Aydin and Ozturk [7] utilized a computerized CFD approach that was assembled and validated against experimental methods for aerating waterways, achieving a balanced compromise between the two techniques. Hasan et al. [8] developed a physical model of the Glaber Dam at a 1:30 scale and gathered data showing that the cavity index never exceeded the critical threshold at any of the experiment's analyzed sites. Hager [9] studied ventilation in chutes with homogeneous flows, demonstrating that the slope of the chute bottom influences the average air concentration in the flow cross-section.

According to Zhang et al. [10], impact forces of up to 300 MPa may be produced by the collapse and recovery of cavitation bubbles. In graded drainage channels, Frizell et al. [11] found a relationship between the flow co-friction factor and the critical cavity index. Parsaie et al. [12] analyzed cavitation processes along a dam's downstream bucket using Flow 3D software, and using a cavitation index of 0.25, they

came to the conclusion that cavitation along a spillway is improbable. Fadaei Kermani et al. [13] employed the fuzzy-near k-algorithm to efficiently and appropriately estimate cavitation damage on dam downstreams. Ghazi et al. [14] also used Flow 3D software to simulate a dam spillway in 3D, finding that the lumen index always exceeded the critical lumen number at all flow rates for a return duration of 1000 years. Barzegari et al. [15] utilized digital flow modeling software on the downstream of a dam and found no occurrence of cavitation at any tested flow rates.

Youssef and Micovic [16] examined a prototype to scale simulation of cavity damage to a new watercourse, noting that factors such as the period of continuous spillage and a higher cavity potential on both smooth concrete surfaces and surfaces with consistently rough edges, as well as sharp blunt stairs related to stages with rounded limits, contributed to cavity damage in this culvert. Samadi-Boroujeni et al.'s modeling work [17] concentrated on the association between fluid channel bed roughness height and lumen index. According to their research, there would be no discernible impact on the cavity index value within a 95% confidence range if the roughness height was reduced from 2.5 to 1 mm.

This study evaluated the amount of concrete abrasion that happens downstream of an ogee spillway using Computational Fluid Dynamics (CFD) through ANSYS Fluent software. The main goal of the study is to evaluate the effectiveness of 3D ANSYS Fluent platforms in simulating flow over an ogee spillway utilizing various water discharges that range from 100 to 717 m^3/s.

2. MATERIAL AND METHODS

Numerical findings have been more popular in recent years as a means of tackling complicated problems that are costly or challenging to complete in the lab [18]. Pre-processing, solution, and post-processing are the three main dependent steps that make up the numerical procedure. Before beginning the next level, each one must be finished exactly as described. These three phases are fully explained in the sections that follow.

2.1 Pre-processing

A real hydraulic structure had to be converted into a model that could be computed as the initial step in numerical modeling. This required meshing, boundary constraints, and the definition of geometry for the numerical domain. Determining the solution domain and grid sizing took up more than 50% of the time spent on CFD modeling [19]. The commercial ANSYS Fluent software is frequently used to solve the continuity and unsteady Reynold Averaged Navier Stokes (RANS) equations for simulating the flow pattern over a spillway. Eqs. (1) and (2) show the standard forms of the continuity and RANS equations:

$$\frac{\partial u_i}{\partial x_i} = 0 \tag{1}$$

$$\frac{\partial u_i}{\partial t} + u_j \frac{\partial u_i}{\partial x_j} = -\frac{1}{\rho}\frac{\partial P}{\partial x_i} + \frac{\partial}{\partial x_j}(2\nu S_{ij} + \tau_{ij}) \tag{2}$$

where, u_j represents the average velocity of the Cartesian components; x_j refers to the Cartesian coordinates (where j=1, 2, 3); P indicates pressure; t stands for time; ρ denotes density; and ν symbolizes dynamic viscosity. The term S_{ij} corresponds to the strain rate tensor, while τ_{ij} refers to the Reynolds stress tensor.

The governing equations of flow across spillways were solved using the Finite Volume Method (FVM) in the ANSYS Fluent software. Within the field of hydraulics, the FVM approach is generally favored over the Finite Difference Method (FDM) and the Finite Element Method (FEM) [20]. This preference is partly because FVM typically requires less computational time than FEM [21]. Additionally, the FVM allows for the use of various mesh types to accurately represent different computational domains, offering flexibility that the structurally constrained mesh required by the FDM does not provide.

Both systems include a variety of turbulence closure models, such as the RNG k–ε, k–ω, and conventional k–ε models. The RNG (k–ε) model is employed in this work to construct models as it is more suited for flows on surfaces with plenty of curves. ANSYS Science Company created the commercial ANSYS Fluent software. The Volume of Fluid (VOF) approach [22, 23] is included in this program to address free surfaces. For treating free surfaces, the water and air interface in the VOF method provides values ranging from one to zero for each cell in the calculation domain [24]. The approach developed by Hirt and Sicilian [25] for precisely defining and entering the model shape into the governing equations is called FAVOR (Fractional Area Volume Obstacle Representation). It should be emphasized that as mesh smoothness grows, so does this method's usefulness. The second platform in the current investigation was the Fluent software created by the ANSYS Company. Due to the long simulation times associated with modeling in three dimensions (3D): the Fluent platform has been employed in the two-dimensional (2D) domain.

Al-Hashimi et al. [26] performed a numerical investigation employing Fluent codes in 2 and 3D to simulate flow over a weir, despite the unfair comparison between the two platforms. Their findings showed that the comparison of 2D results produces reasonable agreements with the 3D domain. A mixture-multiphase-flow model (MMF) and a volume of fluid (VOF) model are the two models that the ANSYS Fluent software uses to accurately depict multiphase flow, respectively. In addition to surface water flow, aeration flows were considered to be influencing factors. The aerated impact in conjunction with the air pressures and the decreasing nappe was also taken into consideration [27, 28]. It was observed that the beginning of venting occurred simultaneously with the formation of a boundary layer in the flow above the ogee spillway. The form of the nap for which the downspout top is intended will abruptly change due to pressure drop brought on by inadequate ventilation.

The primary aim of this study is to examine how different flow rates influence abrasion in an ogee spillway by utilizing the commercial CFD software ANSYS Fluent. To analyze the unsteady Reynolds-Averaged Navier-Stokes (RANS) equations, the RNG k-epsilon turbulence model was applied, along with the Volume of Fluid (VOF) method for tracking the free surface (see Figure 1).

2.2 Geometry and boundary conditions

The necessary hydraulic parameters—such as pressure, velocity, and depth of the water—have been acquired. The

Mandali Dam has been selected as a case study because to its unique contemporary situation, as seen in Figure 2. The Mandali Dam, located in the Diyala Governorate (33°47'4.98"N, 45°35'34.51"E) close to the Iranian border, is one of the most important dams in Iraq. Three million cubic meters of water can fit inside. It was put in place to control floodwaters that came from the Iranian highlands.

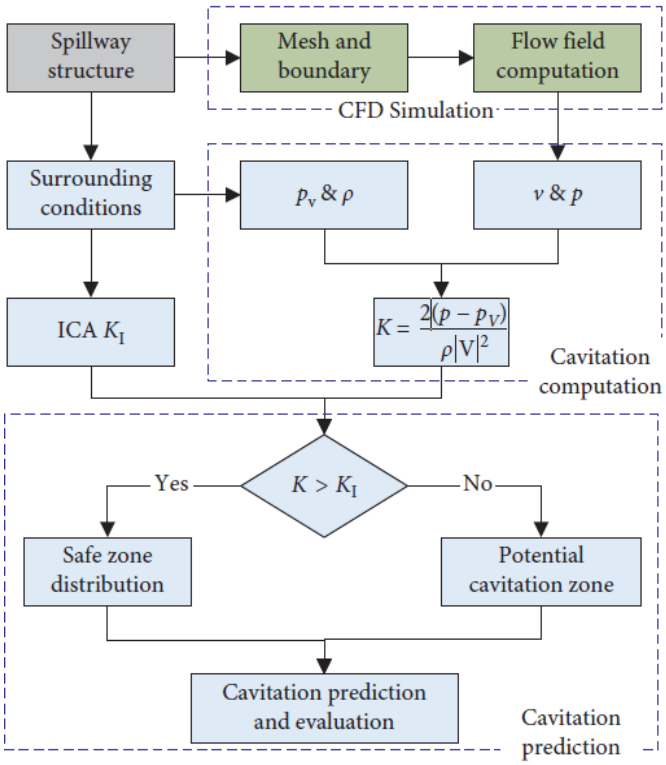

Figure 1. Flowchart methodology for numerical cavitation prediction

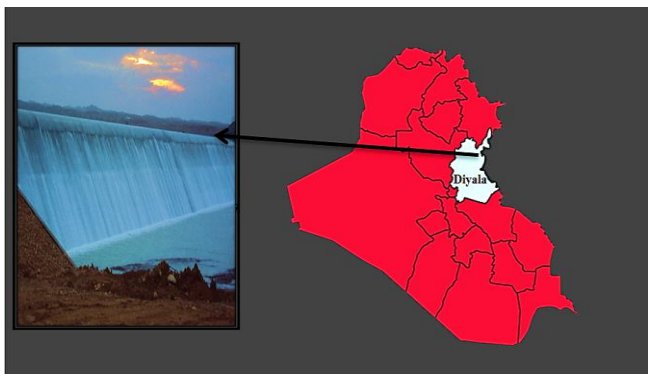

Figure 2. Mandali dam (selected case study)

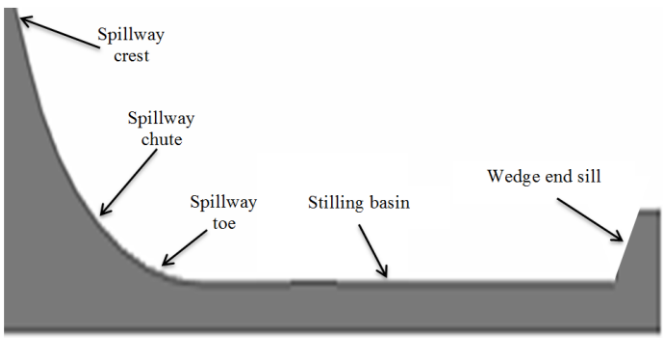

Figure 3. Selected ogee spillway case study model

The CFD model geometry was created using the ANSYS design modeler using the same dimensions as the case study has chosen (Mandali dam). The prototype geometry was constructed using the prototype dimensions for use in numerical modeling. In the stilling basin, an ogee spillway with wedge end sill blocks is installed as the prototype chosen case study, as shown in Figure 3. The chosen ogee channel prototype design characteristics were compiled in Table 1.

Table 1. Dimensions of the model design parameters

Design Elements	Dimensions
Length of crest (m)	42.83
Design discharge (m^3/sec)	398.00
Maximum discharge (m^3/sec)	717.00
Maximum water Head (m)	5.00
Height of spillway (m)	7.80
Design head (m)	3.00
Width of D/S channel (m)	9.00

The surface and body were both frozen in the geometry builder to let a fluid flow via the boundary conditions of the modeling. The geometry and boundaries created for the three-dimensional ogee spillway are shown in Figure 4.

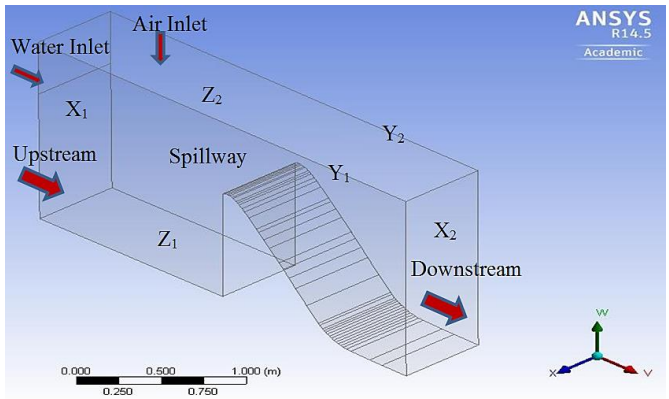

Figure 4. Geometry and boundary condition of ogee spillway model

In the 3D domain, there are six distinct borders (X1, X2, Y1, Y2, Z1, and Z2) that need to be accurately defined, as illustrated in Figure 4. Where Y1, Y2, Z1, and Z2 refer to the right, left, bottom, and top of the spillway, respectively. X1 refers to the spillway upstream; X2 refers to the spillway downstream.

The wall border indicates a non-slip condition, and the outflow (which is determined automatically) shows how much water has flowed from the spillway. Air makes up the top of the domain, hence it was historically described as having a set pressure and a fluid component of zero (free surface). The chosen inflow rate is the upstream boundary condition (X1).

2.3 Meshing

In CFD modeling, mesh construction is an important step that requires careful thought. To examine the fluid flow, the domain had to be split up into smaller cells where the equations that controlled it would be solved. The accuracy of a CFD solution depends on the number of cells in the mesh. As the mesh fineness increases, the answer's accuracy increases as well. The ideal mesh for greater solution precision was obtained by performing several smaller, non-overlapping

computational cells. The finer mesh was used in areas with a high solution interest, whereas the coarser mesh was used in areas with a lower solution interest. The major characteristics in the numerical area of interest are:

-The crest of spillway

-The bottom, where abrasion occurs

-The area where the phases of water and air meet

A fine mesh was used to mesh the areas where water and air were supposed to interact, allowing for a distinct interface, with maximum mesh size 0.01 mm and 0.1 second as a time step sizes used which can affect the reliability of the results. There are numerous choices for 3D meshing, including triangular and quadrilateral meshing. The following definitions of the meshing parameters were used in this investigation [29]:

-Due to its greater ability to produce more accurate findings, a structured grid made up of triangular mesh cells was chosen.

-A refinement was implemented at the spillway crest and in the turbulent region downstream.

-A relevance center and a medium smoothing were also incorporated into the design to provide a steady flow and precise solution.

Five grid sizes of 100, 50, 35, 20, and 10 cm were used for the sensitivity analysis on both platforms. Figure 5(a) demonstrates the ideal mesh size of 10 cm is established using enough accuracy and computing time. Figure 5(b) shows the schematic depiction of model meshing for the build model.

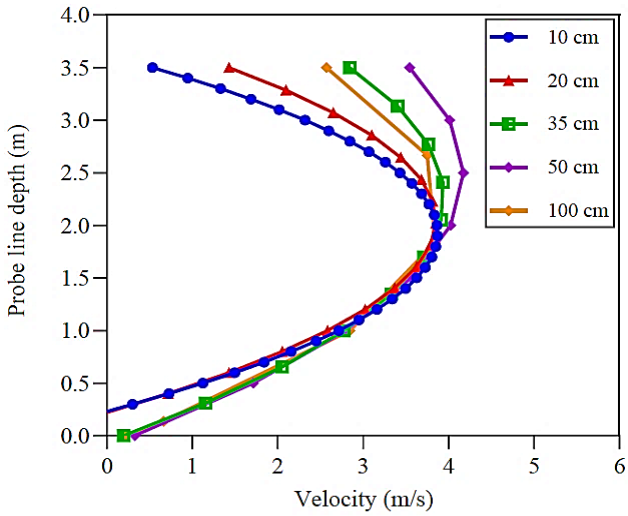

(a)

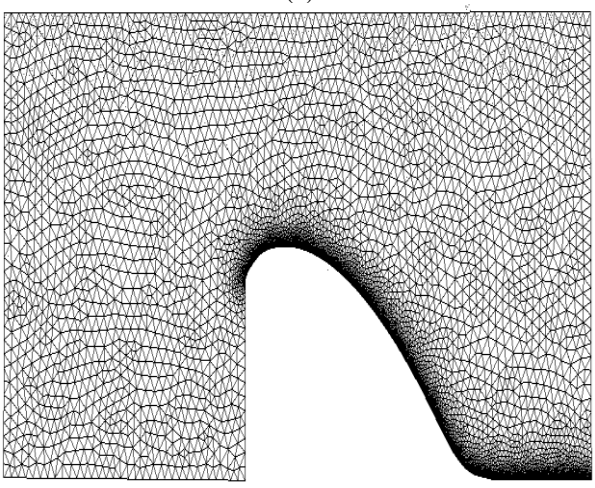

(b)

Figure 5. (a) Mesh sensitivity analysis according; (b) Depiction of the build model geometry meshing

Tetrahedrons, quadrilaterals, and a variety of other shapes can be used to create the mesh for a 3D model. In a different scenario that was examined, tetrahedron meshing was used, but the solution failed because it continued diverging [25]. In order to prevent inadvertent impacts on the accuracy and turnaround time of the computational study, the mesh quality was evaluated. Since they support the kind of study being considered as well as the current problem, the evaluation and assessment of meshing quality in this instance are highly advantageous [20].

2.4 Solver

The model's structure was developed and meshed with the ANSYS Fluent program, and then the mesh was imported into a fluent solver. It was necessary to provide the solver's many parameters before the calculations could start. The following expression $\sigma_i > \sigma$ was utilized to estimate this index:

$$\sigma = \frac{P_0 - P_v}{\rho \frac{V^2}{2}} \tag{3}$$

For a single roughness, the critical cavitation index can be determined using the following equation based on the findings of reference [6]:

$$\sigma_i = \frac{h - h_v}{\frac{V_0^{\,2}}{2g}} \tag{4}$$

where, V_0 is the velocity close to the surface, h_v is the height of the vapor pressure, and h stands for the height of the absolute pressure.

2.5 Post-processing

For the study, five cases of upstream flow rates (depending on water head and velocity values) are selected as simulation scenarios and as illustrated in Table 2.

Table 2. Properties of the spillway upstream Q values

Run	I	II	III	IV	V
Flow rate (m^3/sec)	100	250	400	600	717
Symbols	Q_1	Q_2	Q_3	Q_4	Q_5

The constant downstream channel width was determined by accounting for the varying downstream channel length. The flow rates were taken into consideration while taking into account variations in the unit discharge flow rate (Q) at the apex of the water discharge channel, as indicated in Table 3. Velocity values were calculated for each simulated test using the continuity equation, flow rate, width, and known depth.

Table 3. Performance indicators of the corrosion model

Performance Indicator	Value
Training dataset R^2	0.637
Training dataset RMSE	0.472

As is well known, for free surface flows, which were taken into account as spillways in the present study, the impact of gravity was often more significant than the impact of viscosity and surface tension [6, 30]. The prototypes were therefore

generally based on the Froude (Fr) without taking the viscosity impact into account. When the Reynolds number exceeds a predetermined threshold (=104): this happens.

For all the hydraulic data, including velocity, pressure, and water depth, solutions were run for 20 seconds. Given the knowledge gained from earlier investigations, it is understood that the subjected loads must stabilize over about 20 seconds.

3. RESULTS AND DISCUSSION

3.1 Cavitation index

Data like average velocity and bottom pressure in different areas of the structure were analyzed in order to monitor and control the occurrence of abrasion brought on by the cavitation phenomenon. Eqs. (3) and (4) are utilized to ascertain the optimal measurement for each of the five flow rates and to create the curve of changes in the cavitation indexes along the longitudinal axis of the stream in the simulated model, as depicted in Figure 6.

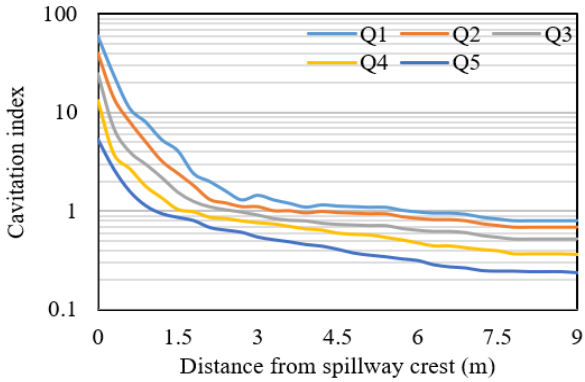

Figure 6. Cavitation along the spillway in numerical simulations with studied flow rate

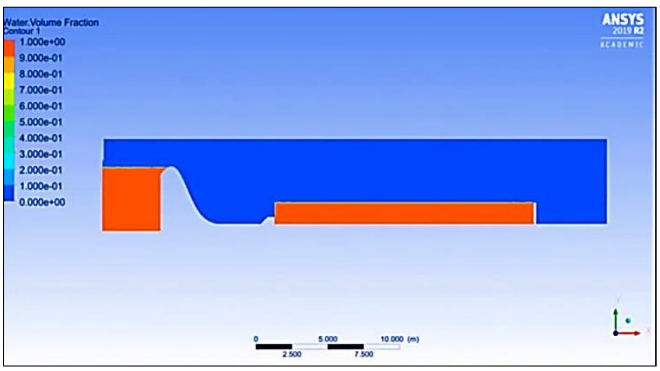

(a) Q_0=0 m^3/sec

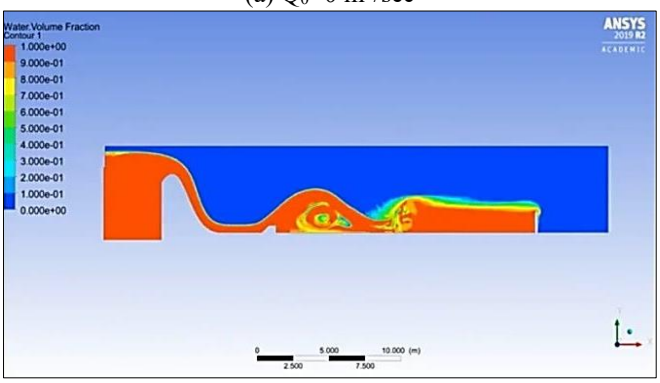

(b) Q_1=100 m^3/sec

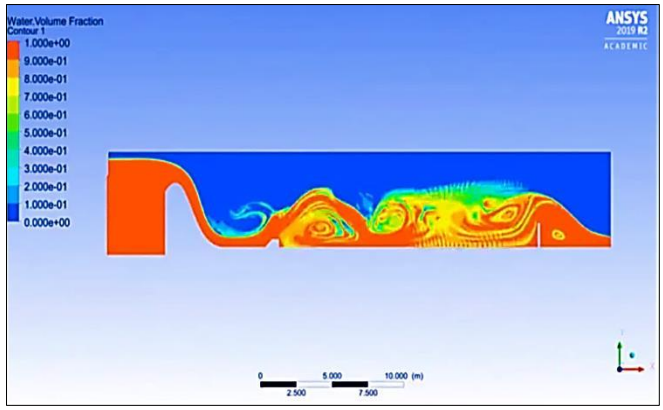

(c) Q_2=250 m^3/sec

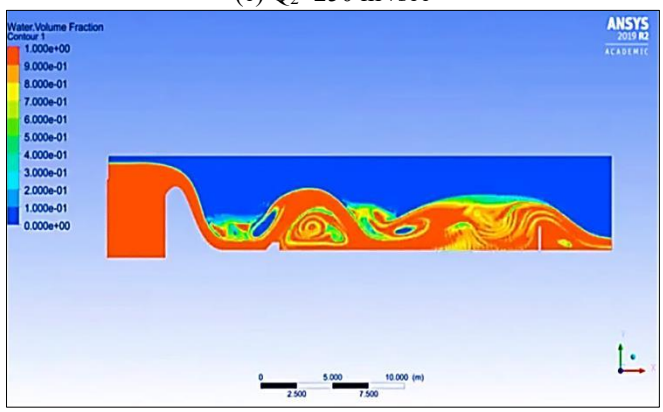

(d) Q_3=400 m^3/sec

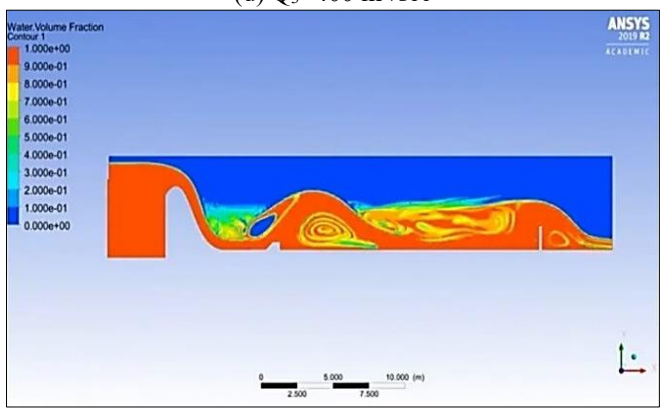

(e) Q_4=600 m^3/sec

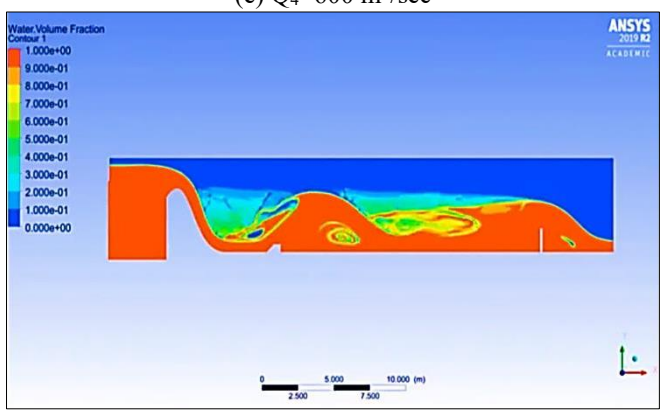

(f) Q_5=717 m^3/sec

Figure 7. Optimal effect of select flow rates

To calculate the cavitation index under optimal flow rate conditions, data were collected from the sidewall and the central axis at various positions, as illustrated in Figure 7(a) to Figure 7(f).

The observations highlighted by Falvey [6] are used to calculate the presence of cavitation in this study. The cavitation index along the Mandali spillway has been observed to decrease according to the cavitation rate curves shown. Figure 6 indicates that cavitation protection is unnecessary for up to 1.5 meters downstream of the spillway crest when the intended flow rate passes over the spillway. However, the cavitation index peaks at 1.8 approximately 3 meters from the spillway crest, after which it begins to decline as the flow velocity increases. This trend continues for 9 meters beyond the spillway crest. Based on recommendations [6], modifications above a dam spillway should involve smoothing out any rough patches on the concrete surface to prevent further reductions in the cavitation index [31-33].

When the flow rate was determined to be the same as the design flux discharge, the cavitation index was found to be less than the critical value (=0.25) between piezometrics 25 and 26, or 8 meters from the end of the flow stream. The lowest cavity index for (100, 250, 400, 600, 717) m^3/s was estimated to be 0.234, 0.363, 0.523, 0.680, and 0.801 at 9 m from the crest, respectively.

The range of the indication calculated in this section of the chute is 1.5 to 0.25. Falvey's suggestions include that modifications should be made to raise the bore index downstream of the dam if a flow rate larger than the planned flow crosses the spillway.

Figures 7(a) to (f) show the variations in the chosen flow-cavitation rates. The pictures demonstrate how, as flow rate increases, the lumen expands, pushing the maximum flow rate indicator value above a crucial threshold at the downstream end of the flow.

Moreover, the cavitation index in the spillway chute ranged from 0.25 to 0.4 at discharges smaller than the design discharge, indicating the necessity for modification through the elimination of imperfections in the chute surface concrete. The outcomes of the numerical models concur in this regard.

3.2 Cavitation index for different roughness heights

The investigation's conclusions and the suggestions [6] dictate that the flow be modified by eliminating unevenness and reducing roughness height. Therefore, a numerical model of ground-state roughness in ANSYS Fluent was calibrated in order to better understand the effect of changing the lubricant's surface on changing the values of the lumen index. This will allow us to modify the spillway surface at the optimal degree of roughness.

In addition to the base roughness height (k_s=2.5 mm): the model was run for roughness height values between 1 and 2 mm under constant hydraulic circumstances of the anticipated flow rate where the cavity index was less than the critical value, and the cavity index was then calculated.

For various roughness height values, Figure 8 illustrates the variations in the cavity index values as a function of distance. The findings show that for roughness heights of 1, 2, and 2.5 mm, the lowest cavity index values are 0.2906, 0.2733, and 0.2471, respectively. This demonstrates that decreasing the roughness height causes the cavity index values to increase, taking them away from the critical value specified by Falvey [6] against the incidence of cavity relative to the base scenario.

To determine the significance level of the influence of roughness height on the cavity index value, the $t-test$ [31, 32] was statistically significant. The study' findings indicate that there is no statistically significant difference in the lumen index for instances with a roughness height of 2.5 and 2 mm at a 95% confidence level. A similar conclusion was reached for cases with a roughness height of 2.5 and 1 mm. These findings show that the modified by reducing irregularities' method, which lowers the height of the ogee stream roughness, would not significantly alter the cavity index value.

The outcomes of mathematical simulation further demonstrate that the mean velocity dropped as the roughness height was decreased. Although increasing flow velocity results from reducing roughness height, any reduction in roughness height also lessens the amount of discharge turbulence. As a result, the viscosity influence increases when flow turbulence is reduced, and flow streamlines become considerably steadier as related to the case with greater turbulence.

Furthermore, the boundary layer's average flow discharge is decreased (Figure 9). The velocity profiles and flow depth were investigated in order to validate the aforementioned point of view. The outcomes demonstrate that lowering the roughness height affected the velocity gradient. Figure 9 displays depth calculations and velocity variations within 90 m of the crest. Figure 9 illustrates how a decrease in roughness height affected the velocity gradient and, ultimately, the average velocity. This decrease causes the cavitation index at the Ogee spillway chute downstream to increase.

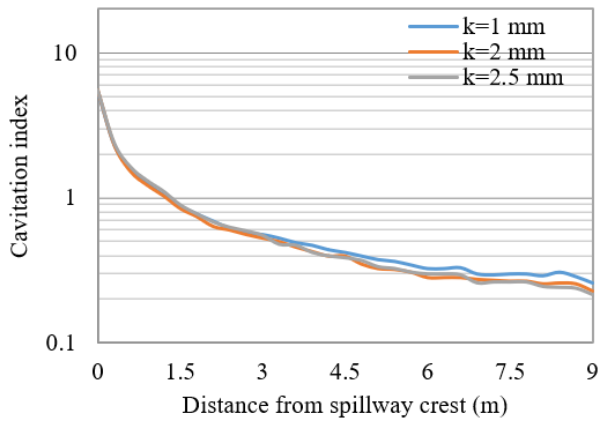

Figure 8. Variation of cavitation index along the spillway for different roughness heights

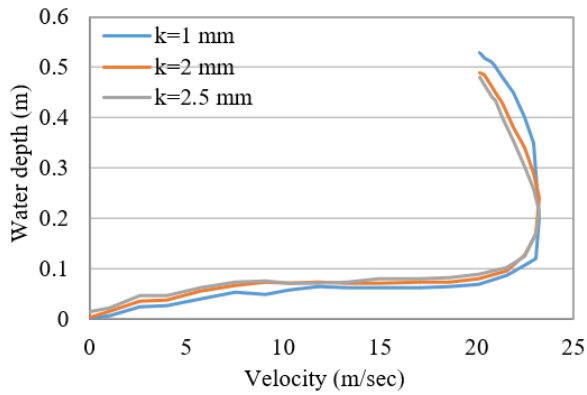

Figure 9. Changes in velocity distribution corresponding to various bed roughness heights.

The input data was used to train the abrasion estimate model. Hager [9] findings, which served as the training and validation data, were then used to validate the model. The abrasion model's performance metrics were chosen to be the

coefficient of repeatability and RMSE. Generally speaking, the coefficient of prediction indicates the percentage of the response variable's variation that the used model can account for.

As a general rule, RMSE values in the range of 0.2 to 0.5 indicate that the model can reasonably predict the data. Furthermore, an adjusted R-squared of greater than 0.75 indicates a high level of accuracy. The present abrasion ratio and the research [9] had a coefficient of determination and RMSE of 0.637 and 0.472, respectively. Consequently, the training and validation datasets' coefficients of determination were more than 0.75. The outcomes of the training and validation are shown in Table 3 and Figure 10.

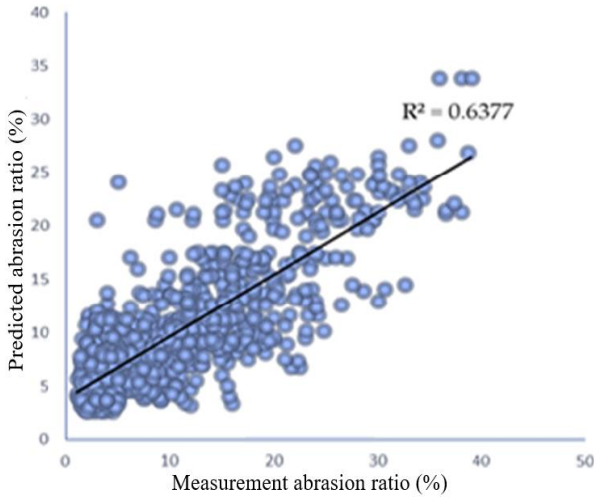

Figure 10. Comparison of abrasion prediction results with the model from the study [9]

3.3 Abrasion thickness under selected flow rates

Based on the numerical simulation, Figures 11(a) to (f) shows the thickness of the abrasion profile in the central plane for the ogee spillway model.

The outcome demonstrates that abrasion starts consistently from the spillway's heel and increases until it reaches the spillway's top. The minimal abrasion in the center plane is approximately 0.25 mm, according to the numerical simulation. By comparing the numerical results, it is possible to omit the minimum value from the experimental abrasion average, which would allow the numerical results to more accurately depict the full distribution of the abrasion effect. For instance, the cavitation index primarily depicts the possibility of hydraulic abrasion occurring in the high-speed flow of water spillway on the concrete surface.

The results also shown that the highest abrasion value occurs at a distance of 1.00 mm from the spillway surface when high velocity flow is occurrence, and this distance is crucial in determining when failure will occur. A key consideration in the construction of hydraulic structures is concrete strength, which is affected by regional imperfections, material qualities, and environmental factors. Typically, the building process and implementation requirements are used to develop the concrete mixture.

Through the results of the current study, we recommend that the hydraulic characteristics of the flow in terms of flow velocity and the height of the water column must be taken into account accurately in the design of such facilities. As well as relying on numerical models because they give completely reliable results in predicting hydraulic phenomena such as cavitation which lead to abrasion of the concrete surface of these structures. This phenomenon is considered dangerous and thus leads to failure in such vital structures that are directly related to human life and the environment, as well as closely linked to the economy since its implementation and maintenance require huge funds estimated at hundreds of dollars.

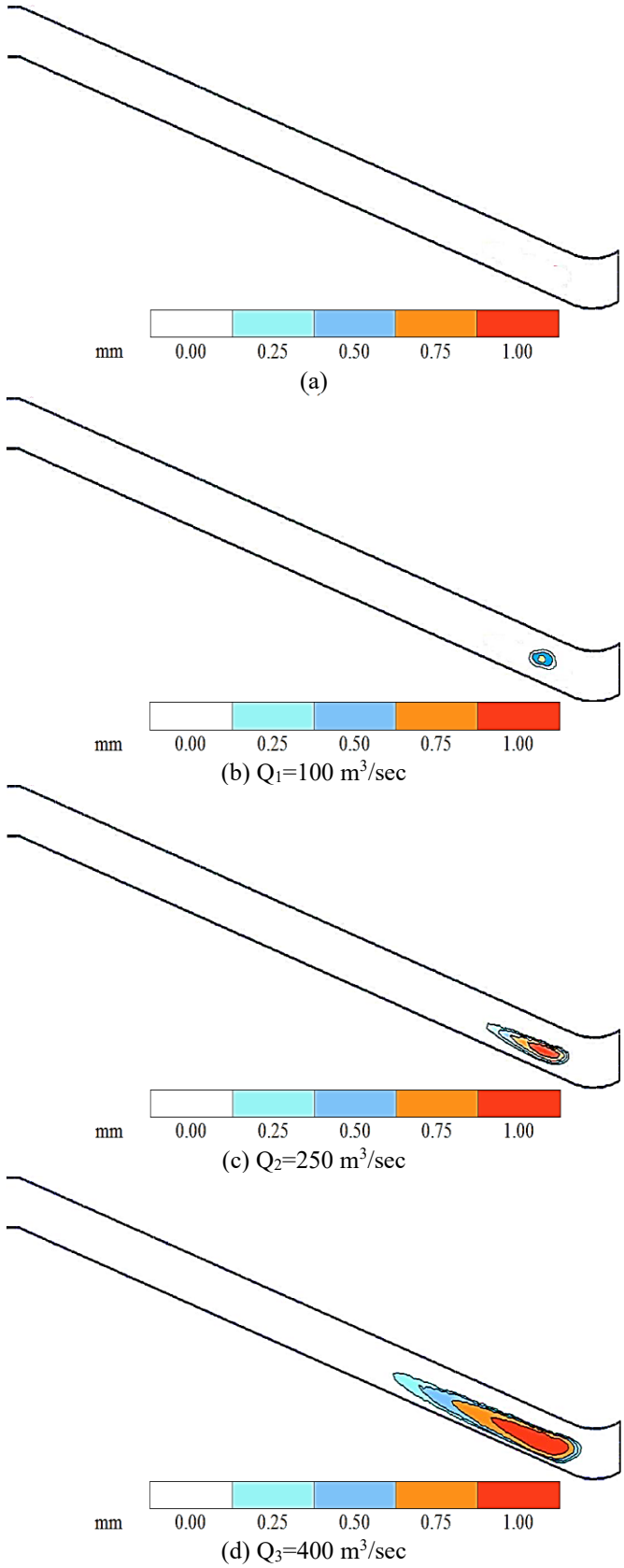

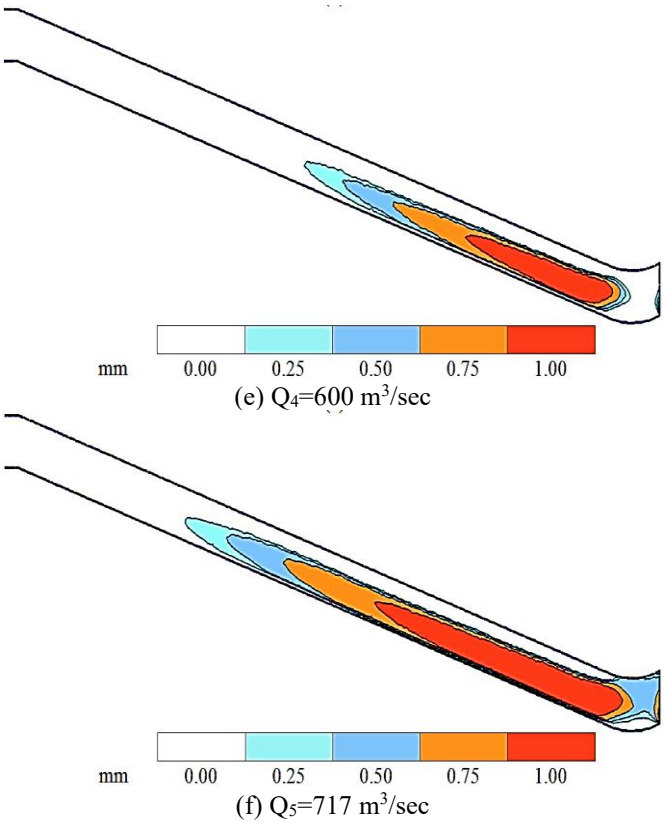

Figure 11. Thickness of potential abrasion zone in the ogee spillway central plane

4. CONCLUSIONS

According to the results of the conducted simulated tests of inflow rate variations along the ogee spillway surface, the main conclusions can be summarized:

1. When the flow rate increases, the cavitation increases proportionally, and thus the amount of abrasion of the spillway concrete surface increases.
2. Decreasing the roughness height affected the gradient of velocity and cavitation index value, which decreased the average velocity, where the largest amount of abrasion occurs with high flow and reaches 1.00 mm at the spillway surface, which significantly contributes to spillway failure with long-term behavior.
3. For roughness heights of 1, 2, and 2.5 mm, the cavitation index's lowest values were 0.2906, 0.2733, and 0.2471, respectively.
4. The spillway crest was found to have the least amount of abrasion, unlike the toe and chute of the spillway, which had a higher amount of abrasion
5. Raising the roughness height causes the cavitation index numbers to rise and diverge from the critical value found in previous research; however, an analysis of statistics of significance showed that a 95% confidence interval would not be affected significantly if the roughness level was reduced from 2.5 to 1 mm.
6. A good validation results of the current study abrasion ratio and the previous study through the coefficient of determination and RMSE were appeared with 0.637 and 0.472, respectively.
7. High flow rates and abrasion risk be considered in spillway design or that surface roughness be optimized to balance cavitation index and average velocity.

REFERENCES

[1] Chanson, H. (1988). Study of air entrainment and aeration devices on spillway model. Doctoral dissertation, University of Canterbury, Christchurch, New Zealand.

[2] Wan, W., Liu, B., Raza, A. (2018). Numerical prediction and risk analysis of hydraulic cavitation damage in a high-speed-flow spillway. Shock and Vibration, 2018(1): 1817307. https://doi.org/10.1155/2018/1817307

[3] Sarwar, M.K., Ahmad, I., Chaudary, Z.A., Mughal, H.U.R. (2020). Experimental and numerical studies on orifice spillway aerator of Bunji Dam. Journal of the Chinese Institute of Engineers, 43(1): 27-36. https://doi.org/10.1080/02533839.2019.1676652

[4] Kramer, K. (2004). Development of aerated chute flow. Doctoral dissertation, ETH Zurich.

[5] Imanian, H., Mohammadian, A. (2019). Numerical simulation of flow over ogee crested spillways under high hydraulic head ratio. Engineering Applications of Computational Fluid Mechanics, 13(1): 983-1000. https://doi.org/10.1080/19942060.2019.1661014

[6] Falvey, H.T. (1990). Cavitation in Chutes and Spillways. Denver, CO, USA: US Department of the Interior, Bureau of Reclamation.

[7] Aydin, M.C., Ozturk, M. (2009). Verification and validation of a computational fluid dynamics (CFD) model for air entrainment at spillway aerators. Canadian Journal of Civil Engineering, 36(5): 826-836. https://doi.org/10.1139/L09-017

[8] Hasan, R.F., Seyedi, M., Alsultani, R. (2024). Assessment of Haditha Dam surface area and catchment volume and its capacity to mitigate flood risks for sustainable development. Mathematical Modelling of Engineering Problems, 11(7): 1973-1978. https://doi.org/10.18280/mmep.110728

[9] Hager, W.H. (1991). Uniform aerated chute flow. Journal of Hydraulic Engineering, 117(4): 528-533. https://doi.org/10.1061/(ASCE)0733-9429(1991)117:4(528)

[10] Zhang, H., Han, B., Yu, X.G., Ju, D.Y. (2013). Numerical and experimental studies of cavitation behavior in water-jet cavitation peening processing. Shock and Vibration, 20(5): 895-905. https://doi.org/10.3233/SAV-130792

[11] Frizell, K.W., Renna, F.M., Matos, J. (2013). Cavitation potential of flow on stepped spillways. Journal of Hydraulic Engineering, 139(6): 630-636. https://doi.org/10.1061/(ASCE)HY.1943-7900.0000715

[12] Parsaie, A., Dehdar-Behbahani, S., Haghiabi, A.H. (2016). Numerical modeling of cavitation on spillway's flip bucket. Frontiers of Structural and Civil Engineering, 10: 438-444. https://doi.org/10.1007/s11709-016-0337-y

[13] Fadaei Kermani, E., Barani, G. A., Ghaeini-Hessaroeyeh, M. (2018). Cavitation damage prediction on dam spillways using Fuzzy-KNN modeling. Journal of Applied Fluid Mechanics, 11(2): 323-329. https://doi.org/10.29252/jafm.11.02.28356

[14] Ghazi, B., Daneshfaraz, R., Jeihouni, E. (2019). Numerical investigation of hydraulic characteristics and prediction of cavitation number in Shahid Madani Dam's Spillway. Journal of Groundwater Science and Engineering, 7(4): 323-332. https://doi.org/10.19637/j.cnki.2305-7068.2019.04.003

[15] Barzegari, M., Sobhkhiz Foumani, R., Isari, M., Tarinejad, R., Alavi, S. A. (2019). Numerical investigation of cavitation on spillways. A case study: Aydoghmush dam. Journal of Numerical Methods in Civil Engineering, 4(1): 1-9. https://doi.org/10.52547/nmce.4.1.1
[16] Yusuf, F., Micovic, Z. (2020). Prototype-scale investigation of spillway cavitation damage and numerical modeling of mitigation options. Journal of Hydraulic Engineering, 146(2): 04019057. https://doi.org/10.1061/(ASCE)HY.1943-7900.0001671
[17] Samadi-Boroujeni, H., Abbasi, S., Altaee, A., Fattahi-Nafchi, R. (2020). Numerical and physical modeling of the effect of roughness height on cavitation index in chute spillways. International Journal of Civil Engineering, 18: 539-550. https://doi.org/10.1007/s40999-019-00479-2
[18] Mohammed, J.R., Noori, B.M.A., Hussein, I.A. (2017). Modeling of the hydraulic performance of ogee spillway using computational fluid dynamics (CFD). Journal of Duhok University, 638-653.
[19] Yildiz, A., Yarar, A., Kumcu, S.Y., Marti, A.I. (2020). Numerical and ANFIS modeling of flow over an ogee-crested spillway. Applied Water Science, 10(4): 90. https://doi.org/10.1007/s13201-020-1177-4
[20] Alsultani, R., Karim, I.R., Khassaf, S.I. (2022). Mathematical formulation using experimental study of hydrodynamic forces acting on substructures of coastal pile foundation bridges during earthquakes: As a model of human bridge protective. Res Militaris, 12(2): 6802-6821.
[21] Salmasi, F., Abraham, J. (2022). Discharge coefficients for ogee spillways. Water Supply, 22(5): 5376-5392. https://doi.org/10.2166/ws.2022.129
[22] Hirt, C.W., Nichols, B.D. (1981). Volume of fluid (VOF) method for the dynamics of free boundaries. Journal of Computational Physics, 39(1): 201-225. https://doi.org/10.1016/0021-9991(81)90145-5
[23] Kim, D.G., Park, J.H. (2005). Analysis of flow structure over ogee-spillway in consideration of scale and roughness effects by using CFD model. KSCE Journal of Civil Engineering, 9: 161-169. https://doi.org/10.1007/BF02829067
[24] Bayon, A., Toro, J.P., Bombardelli, F.A., Matos, J., López-Jiménez, P.A. (2018). Influence of VOF technique, turbulence model and discretization scheme on the numerical simulation of the non-aerated, skimming flow in stepped spillways. Journal of Hydro-Environment Research, 19: 137-149. https://doi.org/10.1016/j.jher.2017.10.002
[25] Hirt, C.W., Sicilian, J.M. (1985). A porosity technique for the definition of obstacles in rectangular cell meshes. In International Conference on Numerical Ship Hydrodynamics, 4th, Washington, DC, USA.
[26] Al-Hashimi, S.A., Madhloom, H.M., Khalaf, R.M., Nahi, T.N., Al-Ansari, N.A. (2017). Flow over broad crested weirs: Comparison of 2D and 3D models. Journal of Civil Engineering and Architecture, 11(8): 769-779. https://doi.org/10.17265/1934-7359/2017.08.005
[27] Alsultani, R., Khassaf, S.I. (2022). Nonlinear dynamic response analysis of coastal pile foundation bridge pier subjected to current, wave and earthquake actions: As a model of civilian live. Res Militaris, 12(2): 6133-6148.
[28] Hong, S.H., Sturm, T.W., González-Castro, J.A. (2018). Transitional flow at low-head ogee spillway. Journal of Hydraulic Engineering, 144(2): 04017062. https://doi.org/10.1061/(ASCE)HY.1943-7900.0001398
[29] Muhsun, S.S., Al-Sharify, Z.T. (2018). Experimental work and CFD model for flowrate estimating over ogee spillway under longitudinal slope effect. International Journal of Civil Engineering and Technology, 9(13): 430-439.
[30] Al-Sultani, R.A.A.A., Salahaldain, Z., Naimi, S. (2023). Features of monthly precipitation data over Iraq obtained by TRMM satellite for sustainability purposes. Al-Mustaqbal Journal of Sustainability in Engineering Sciences, 1(2): 1-16. https://doi.org/10.62723/2959-5932.1001
[31] Rajaa, A.I., Kamela, A.H. (2020). Performance study of fluent-2D and flow-3D platforms in the CFD modeling of a flow pattern over ogee spillway. Anbar Journal of Engineering Sciences, 11(2): 221-230. https://doi.org/10.37649/aengs.2020.171262
[32] Ismael, M.N., Yahya, F.H. (2024). Enhanced concentration control in electrochemical reactors using fuzzy logic with conventional PID and PI controllers. International Journal of Computational Methods and Experimental Measurements, 12(2): 147-153. https://doi.org/10.18280/ijcmem.120204.
[33] Jimenez-Palomino, W.H., Soto-Juscamayta, L.M., Ccatamayo-Barrios, J.H., Bendezú-Prado, J.L., Berrocal-Argumedo, K., Esparta-Sanchez, J.A., Maldonado-Llacua, G.M., Mayorga-Rojas, J.C., Romero-Baylon A.A. (2024). Implementation of a GIS for the conservation of irrigation canals: Using ArcGIS and Python for automation. Mathematical Modelling of Engineering Problems, 11(9): 2337-2346. https://doi.org/10.18280/mmep.110907